

## Two EPR-detectable [4Fe–4S] clusters, N2a and N2b, are bound to the NuoI (TYKY) subunit of NADH:ubiquinone oxidoreductase (Complex I) from *Rhodobacter capsulatus*

Mireille Chevallet<sup>a</sup>, Alain Dupuis<sup>a</sup>, Jean-Paul Issartel<sup>b</sup>, Joël Lunardi<sup>a</sup>,  
Ronald van Belzen<sup>c</sup>, Simon P.J. Albracht<sup>c,\*</sup>

<sup>a</sup>BECP/DBMS/CEA Grenoble, EMI INSERM 9931, 17 Av des Martyrs, F-38054 Grenoble Cedex 09, France

<sup>b</sup>CNRS and Genome express, 11 chemin des près, F-38944 Meylan, France

<sup>c</sup>Swammerdam Institute for Life Sciences, Biochemistry, University of Amsterdam, Plantage Muidergracht 12, NL-1018 TV Amsterdam, The Netherlands

Received 29 August 2002; received in revised form 9 December 2002; accepted 10 December 2002

### Abstract

NADH:ubiquinone oxidoreductases (Complex I) contain a subunit, TYKY in the bovine enzyme and NuoI in the enzyme from *Rhodobacter capsulatus*, which is assumed to bind two [4Fe–4S] clusters because it contains two sets of conserved cysteine motifs similar to those found in the 2[4Fe–4S] ferredoxins. It was recently shown that the TYKY subunit is not an ordinary 2[4Fe–4S] ferredoxin, but has a unique amino acid sequence, which is only found in NAD(P)H:quinone oxidoreductases and certain membrane-bound [NiFe]-hydrogenases expected to be involved in redox-linked proton translocation [FEBS Lett. 485 (2000) 1]. We have generated a set of *R. capsulatus* mutants in which five out of the eight conserved cysteine residues in NuoI were replaced by other amino acids. The resulting mutants fell into three categories with virtually no, intermediate or quite normal Complex I activities. EPR-spectroscopic analysis of the membranes of the C67S and C106S mutants, two mutants belonging to the second and third group, respectively, showed a specific 50% decrease of the EPR signal attributed to cluster N2. It is concluded that the NuoI (TYKY) subunit binds two clusters N2, called N2a and N2b, which exhibit very similar spectral features when analyzed by X-band EPR spectroscopy.

© 2002 Elsevier Science B.V. All rights reserved.

**Keywords:** NADH:ubiquinone oxidoreductase; Complex I; NuoI; TYKY; Iron–sulfur cluster N2; *R. capsulatus*

### 1. Introduction

NADH:ubiquinone oxidoreductase (EC 1.6.5.3; Complex I) is an integral membrane protein present in the inner membrane of mitochondria and in the plasma membrane of many microorganisms. It catalyzes electron transfer from NADH to ubiquinone in a process coupled to the ejection of protons over the membrane. In purple bacteria, when anaerobically growing in the light, Complex I is required for the production of NADH by the reduction of NAD<sup>+</sup> with electrons from the quinone pool in a reaction driven by the proton-motive force. The NADH is converted to NADPH via a transhydrogenase and then the reducing equivalents are used for CO<sub>2</sub> fixation.

The mitochondrial enzyme consists of at least 43 subunits and has a molecular mass of over 900 kDa [1,2]. The bacterial enzymes are simpler, but still minimally contain 13 subunits [3]. While a crystal structure is not available, electron-microscopic studies revealed an L-shaped form for the enzyme [4–6], although recently a horseshoe structure was proposed as the native form of the enzyme from *Escherichia coli* [7]. Electron transfer from NADH to ubiquinone is facilitated by a number of prosthetic groups: FMN and iron–sulfur (Fe–S) clusters.

When reduced with NADH, the bovine enzyme shows four major EPR signals. They have been ascribed to Fe–S clusters: one signal from a binuclear ([2Fe–2S]) cluster known as N1b and three signals from tetranuclear ([4Fe–4S]) clusters, called N2, N3 and N4. Complex I contains an additional 2Fe cluster (N1a), which is not reduced by NADH in the membrane-bound bovine enzyme or the Hatefi-type purified Complex I [8,9]. The properties of

Abbreviations: TTFA, 2-thenoyltrifluoroacetone

\* Corresponding author. Tel.: +31-20-525-5130; fax: +31-20-525-5124.

E-mail address: [asiem@science.uva.nl](mailto:asiem@science.uva.nl) (S.P.J. Albracht).

these clusters in the membrane preparations, as well as some minor additional EPR signals in the purified Complex I, have long been known [9–13].

The precise localization of the several clusters has been studied by a number of groups. In early studies, the purified bovine Complex I was dissected with the help of chaotropic agents and the subcomplexes were studied [14]. More recent studies were focussed on the enzymes from *Paracoccus denitrificans*, *E. coli* and *Rhodobacter capsulatus* (for overviews, see Refs. [3,15,16] and J. Bioenerg. Biomembranes 33 (2001)). Also, the enzymes from the fungus *Neurospora crassa* [17] and the yeast *Yarrowia lipolytica* [18–21] are under intensive study.

Analyses of the primary structures of the Complex I subunits from bovine heart [1,22,23], *P. denitrificans* [24] and *R. capsulatus* [16] have revealed five subunits with potential binding motifs for iron–sulfur clusters. The bacterial subunits called NuoB, NuoE, NuoF, NuoG and NuoI in *R. capsulatus* (or Nqo6, Nqo2, Nqo1, Nqo3 and Nqo9 in *P. denitrificans*) are the equivalents of the PSST, 24-kDa, 51-kDa, 75-kDa and TYKY subunits in the bovine mitochondrial Complex I [22], respectively. The PSST subunit (or NuoB) contains four conserved cysteine residues when compared to homologous subunits and may be able to bind one [4Fe–4S] cluster. This PSST subunit shows a large similarity with the small subunit of [NiFe]-hydrogenases [25,26], which holds a 4Fe cluster located close to the Ni–Fe site [27,28]. It has also been proposed to contain a flavodoxin fold [29], which may bind the second FMN in the bovine enzyme (Ref. [30], accompanying paper). The 75-kDa subunit (or NuoG) is believed to bind two [4Fe–4S] clusters and one [2Fe–2S] cluster [22]. The N-terminal part of this subunit strongly resembles the N-terminal part of the H-cluster-containing subunit of some [Fe]-hydrogenases [11]. This resemblance suggests that one of the 4Fe clusters might have a His ligand, just like one of the 4Fe clusters in the [Fe]-hydrogenase-I from *Clostridium pasteurianum* [31]. Yano et al. [32] have proposed that the clusters N4 and N1b are located in the overexpressed *P. denitrificans* Nqo3 subunit (the equivalent of the 75 kDa subunit). Albracht and De Jong [11] have proposed that the bovine 75-kDa subunit contains two clusters N4 (N4a and N4b) as well as the NADH-nonreducible 2Fe cluster (N1a). The 24-kDa subunit (NuoE or Nqo2) contains a conserved four-Cys motif for the binding of one [2Fe–2S] cluster. This cluster was tentatively assigned to cluster N1a on the basis of experimental evidence derived with the overexpressed Nqo2 subunit from *P. denitrificans* [33,34] or to cluster N1b based on the EPR properties of the overexpressed bovine 24 kDa subunit [35]. Experiments with overexpressed Nqo1 of *P. denitrificans* led Yagi's group to infer that cluster N3 is bound to the 51-kDa subunit [34]. The latter result agrees with the conclusion drawn from in vivo mutagenesis experiments carried out by Fecke et al. [36]. As reported by these authors, after disruption of

the 51-kDa gene in *N. crassa*, Complex I was partially assembled except for the 51-kDa subunit and still contained all redox centres but for FMN and cluster N3. Finally, cluster N2, a cluster that may play a central role in proton translocation [11,29,37,38], was initially assumed to be bound to the TYKY subunit [39]. Yano et al. [40] were the first to show that the Nqo9 (TYKY) subunit indeed contains two EPR-detectable [4Fe–4S] clusters. A shortened version of the Nqo9 (TYKY) subunit from *P. denitrificans* was overexpressed, purified and supplemented with Fe and sulfide. EPR spectra showed two axial signals; one of them had  $g$  values ( $g_{xyz}$  = 1.92, 1.92, 2.05) reminiscent to those of cluster N2. The redox potential of the species were, however, very low ( $< -600$  mV). Other groups [17,20,41] have proposed that cluster N2 is located in the PSST subunit. This was based on the interpretation of effects from point mutations in analogues of the PSST and 49-kDa subunits in *Y. lipolytica*, *N. crassa* and *E. coli* on the EPR spectra of the purified Complex I.

There has been a long-standing dispute about the precise number of these prosthetic groups. In the bovine enzyme, the EPR signals ascribed to the clusters N2, N3 and N4 receive equal contributions from two independent paramagnetic clusters. The cluster N2a, N3a and N4a are specifically reducible with NADPH, while all clusters, N2a, N2b, N3a, N3b, N4a and N4b plus one of the 2Fe clusters (N1b), are reduced by NADH [42]. The spin concentration of the cluster N1b was found to be half the concentration of the clusters N2a+N2b and half the concentration of FMN [43,44]. This was the basis for the proposal that the functional unit of bovine Complex I must contain two FMN groups and eight Fe–S clusters [11,29]. It was recently shown (Ref. [30], accompanying paper) that the routine protein-determination methods overestimate the protein content of the bovine Complex I by between 1.3 and 2.1 times. Based on quantitative analyses of the amino acids, FMN and the EPR signal ascribed to the clusters N2, it was shown that the bovine enzymes used contained at least 1.3–1.4 mol FMN per mole of enzyme and 1.3–1.6 cluster N2. For the classical purified enzyme preparations, an FMN content of 1.2–1.5 nmol FMN per milligram of protein [8,45–48] was reported, i.e. 1.1–1.35 mol of FMN per mole of enzyme of 900 kDa. As the protein content was largely overestimated by the colorimetric methods (Ref. [30], accompanying paper) used in these studies, the FMN content and the total spin concentration from the Fe–S clusters of the bovine enzyme (3.4–4 spins per FMN [9,11]) are adequate for an enzyme with two FMN groups, two [2Fe–2S] clusters, one of which (N1a) is not reducible by NADH, and six [4Fe–4S] clusters.

The present paper deals with the [4Fe–4S] clusters expected to be present in the NuoI (TYKY) subunit of *R. capsulatus* [39]. Effects of point mutations of the

conserved Cys residues in the NuoI subunit on the growth characteristics (both anaerobically in the light and aerobically in the dark) are reported. EPR studies of the Complex I in its most mature state, namely as present in the plasma membranes from *R. capsulatus*, demonstrate the presence of two cubane clusters in the TYKY subunit. Both clusters equally contribute to the EPR signal thus far ascribed to ‘the cluster N2’. The results are incompatible with the interpretation from other laboratories [17,18,20] of the effects of point mutations in homologues of the PSST and 49 kDa subunits in *N. crassa* and *Y. lipolytica* on the properties of the purified Complex I, namely that the 17 K axial EPR signal ( $g_{\text{xyz}} = 2.05, 1.92, 1.92$ ) is due to only one cluster (N2), which is bound to the NuoB (PSST) subunit of Complex I.

## 2. Materials and methods

### 2.1. Mutant generation and bacterial growth

The reference strains from *R. capsulatus* were the B10 and W1 strains. The W1 strain was derivatized from the B10 strain after disruption of the *urf7* gene and the subsequent insertion of a kanamycin-resistance cassette. *Urf7* is an unidentified reading frame of the *nuo* operon located immediately downstream of the *nuoI* gene, which encodes the equivalent of the bovine TYKY subunit. The generation of the W1 strain has been described in detail by Chevallet et al. [49]. Recombinant mutants were generated by chromosomal replacement of the *HindIII* fragment encompassing the second half of the *nuoI* gene according to procedures described for the generation of the W1 or C74S mutant strains [49]. Complementation mutants were obtained after the introduction of a plasmid (pRK415) driving the expression of a mutated form of the *nuoI* gene into the  $\Delta\text{nuoI}$  strain, a strain that has a disrupted *nuoI* gene and a kanamycin-resistance cassette inserted into *urf7*. The  $\Delta\text{nuoI}$  strain was shown to produce quite normal amounts of expressed NuoI subunit as well as a considerable Complex I activity (up to 70% of the wild-type activity) when complemented with the pRK415 vector containing a wild-type copy of the *nuoI* gene [49]. Table 1 summarized the strains used in this paper.

All the strains and mutants were grown at 30 °C in RCV medium [50] complemented with 30 mM sodium lactate as a carbon source. Anaerobic, photosynthetic growth conditions were maintained in liquid cultures by top-filling tubes with de-aerated medium before gas-tight capping and keeping the cultures under permanent neon white light. Dark, aerobic growth in liquid medium was conducted in vigorously shaken flasks. Growth kinetics were followed by measurement of the turbidity of the cultures using a 2100N turbidimeter (Hach, Loveland, USA). Cell densities were expressed as NFU (nephelometer units).

Table 1

*R. capsulatus* strains used in this study

B10	Wild-type reference	[71]
W1	<i>urf6::K1XX</i> mutant strain (Kmr)	[49]
$\Delta\text{nuoI}$	( $\Delta\text{nuoI}$ , <i>urf6</i> )::K1XX mutant strain (Kmr)	[49]
$\Delta\text{nuoI.c}$	$\Delta\text{nuoI}$ complemented by plasmid pRK415- <i>nuoI</i> (Kmr, Tetr)	[49]
<i>Point mutants constructed in W1 genetic background</i>		
C74S	point mutation in chromosomal <i>nuoI</i> gene: Cys-74 → Ser	[49]
I104V	point mutation in chromosomal <i>nuoI</i> gene: I-104 → Val	[49]
C70S	point mutation in chromosomal <i>nuoI</i> gene: Cys-70 → Ser	this study
E71K	point mutation in chromosomal <i>nuoI</i> gene: Glu-71 → Lys	this study
C106S	point mutation in chromosomal <i>nuoI</i> gene: Cys-106 → Ser	this study
<i>Point mutants constructed in <math>\Delta\text{nuoI.c}</math> genetic background</i>		
C67S	point mutation in plasmid born <i>nuoI</i> gene: Cys-67 → Ser	this study
C67R	point mutation in plasmid born <i>nuoI</i> gene: Cys-67 → Arg	this study
C64S	point mutation in plasmid born <i>nuoI</i> gene: Cys-64 → Ser	this study
C64R	point mutation in plasmid born <i>nuoI</i> gene: Cys-64 → Arg	this study

### 2.2. Preparation of plasma membranes

Cells were aerobically grown in the dark in RCV-lactate medium and were harvested by centrifugation at the end of the exponential phase. The cells were suspended in one tenth of the initial volume in buffer A (50 mM HEPES at pH 7.5, 1 mM EDTA, supplemented with 1 mM  $\beta$ -mercaptoethanol, 2  $\mu\text{g/ml}$  aprotinin, 1  $\mu\text{g/ml}$  antipain, 1  $\mu\text{g/ml}$  leupeptin, 1  $\mu\text{g/ml}$  chymostatin, 0.5  $\mu\text{g/ml}$  pepstatin). Cells were disrupted by passing through a cell disrupter (Constant Systems, Warwick, UK) at a pressure of 1 kbar. Unbroken cells and large debris were eliminated by centrifugation for 15 min at  $25,000 \times g$ . Membranes were then pelleted by centrifugation of the supernatant for 2 h at  $230,000 \times g$ . The membranes were resuspended in buffer A at a final concentration of 30–50 mg protein/ml and stored in liquid nitrogen until use. For kinetic measurements, the membranes were diluted in 50 mM HEPES and 2 mM EDTA (pH 7.5).

### 2.3. EPR spectroscopy

EPR spectroscopy, simulations and quantifications were performed as described in the accompanying paper [30]. Substrate-induced reduction of the redox groups in the membrane samples, prepared as described above, was conducted as follows (unless stated otherwise): 0.3 ml membrane suspension in an EPR tube was pre-incubated with 0.2 mM TTFA (2-thenoyltrifluoroacetone) and 40 mM fumarate

for 30 min on ice. Then, NADH (4 mM final concentration) was added and the sample was frozen in liquid nitrogen after a further 2 min on ice.

#### 2.4. Miscellaneous methods

SDS polyacrylamide gel electrophoresis and immuno detection were performed as described [49]. NADH oxidase, succinate oxidase and NADH-ferricyanide oxidoreductase activities were assayed as previously reported [51]. Protein concentrations were assayed by the bicinchoninic acid method, using BSA as a standard.

### 3. Results

#### 3.1. Generation of *nuoI* mutants

We have generated seven *R. capsulatus* *nuoI* point mutants in order to assess the NuoI subunit both for the presence and the type of the putative bound iron–sulfur cluster(s). Four Cys residues expected to be involved in the coordination of iron–sulfur clusters have been modified in the present work. Another point-mutant (C74S) and the  $\Delta$ *nuoI* strain were used as strains deficient in Complex I,

while a I104V strain functioned as a control; these three strains have been previously generated [49].

As shown in Fig. 1, the Cys residues belong either to the first motif of four Cys residues (C64, C67, C70, C74) or to the second one (C106). Cys residues were converted into Ser residues and also into Arg residues in the specific cases of Cys 64 and 67. Another mutant was created by converting Glu residue 71 into a Lys residue. Mutants were generated either by substitution of a point-mutated *nuoI* gene for the wild-type chromosomal *nuoI* gene (C70S, E71K, C106S mutants) or by episomal complementation of the *nuoI* deleted strain ( $\Delta$ *nuoI*) with an expression plasmid containing the mutated *nuoI* gene (C64R, C64S, C67R, C67S mutants).

#### 3.2. Immunochemical detection of NuoI

Because substitution of the Cys residue 74 into Ser resulted in dramatic effects on the assembly of the whole multimeric Complex I in *R. capsulatus* [49], we first screened the different mutants for the presence or absence of any expressed NuoI subunit in their membranes. Immunochemical detection of the NuoI subunit was performed on blots of membrane proteins separated on SDS polyacrylamide gels using an anti-NuoI antibody, which targets the C terminus of the subunit. This analysis conclusively indicated

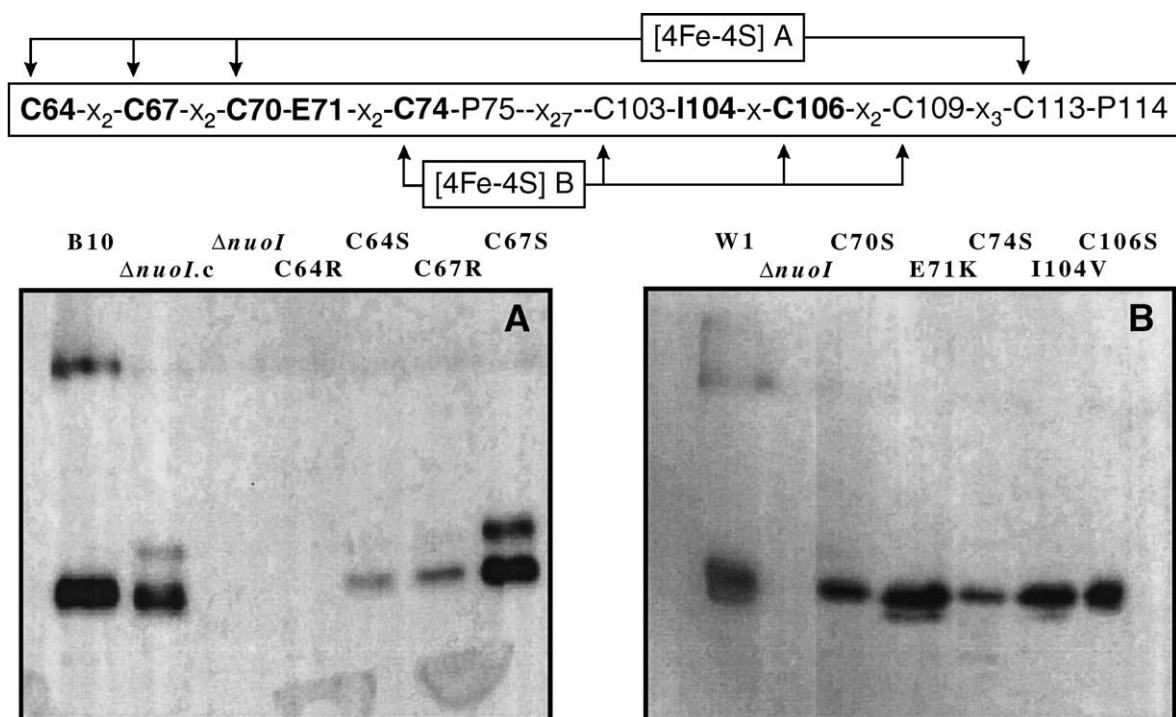


Fig. 1. Immunodetection of the NuoI subunit in the membranes of the different NuoI mutants. Top: Representation of the sequence of the two four-Cys motifs. The mode of binding of the two putative [4Fe–4S] clusters is indicated. Residues targeted by point mutations are in bold. Bottom: Western blot of membranes of the different mutants after separation in an SDS polyacrylamide gel. Immunodetection was performed with an anti-NuoI antibody. The doublet observed in some of the lanes correspond to oxidation artefacts of the Cys of the NuoI subunits. In the case of the  $\Delta$ *nuoI.c* and C67S mutants, the upper band probably corresponds to a larger NuoI subunit resulting from the start of the transduction at an upstream in-phase site, which is present in the transcript of the *nuoI* gene cloned in the expression plasmid only. Quantitative estimates have shown that in the C74S mutant, the NuoI subunit in the membranes generally amounted to less than 20% the quantity of NuoI subunit in the W1 strain [49].



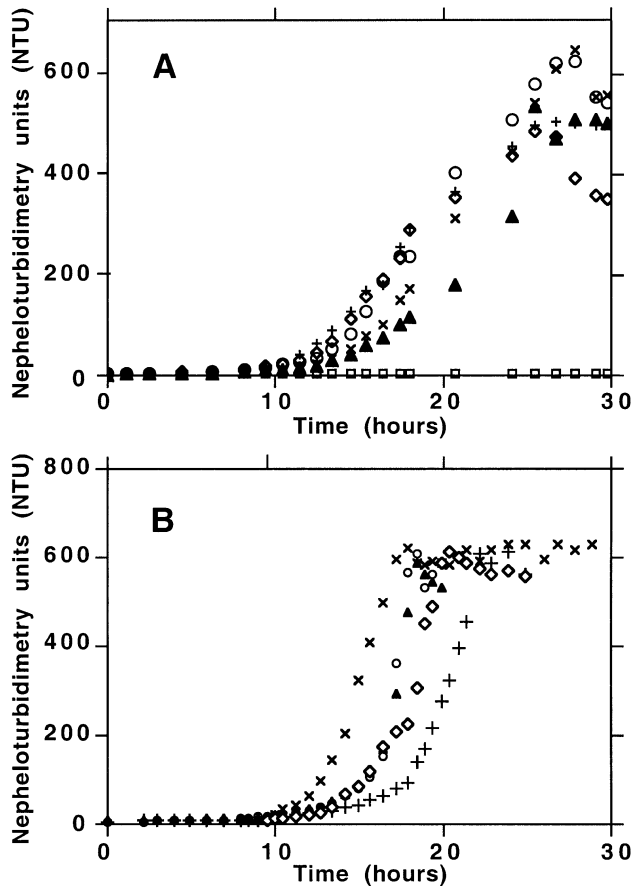


Fig. 2. Comparison of the growth phenotype of the different strains. Growth kinetics were measured as described in Materials and methods in RCV-lactate medium either under anaerobic, photosynthetic conditions (A) or in the dark and under aerobic conditions (B). (+) mutant C67S; (x) mutant C70S; (o) mutant E71K; (□) mutant C74S; (▲) mutant C106S; (◇) wild-type reference (B10).

that the amounts of detectable NuoI subunit in the membranes of the C64R, C64S and C67R mutants were very limited in comparison to the amounts found in the B10 and W1 strains (Fig. 1). Low amounts of NuoI were detected in the C70S and C74S strains while normal amounts of this

subunit were found in the membranes of the C67S, E71K, I104V and C106S strains (Fig. 1).

### 3.3. Growth characteristics

We previously consistently observed that all mutants in which one of the *nuo* genes was disrupted, or a NuoI mutant with a C74S substitution, failed to grow under photosynthetic, anaerobic conditions. The W1 and I104V mutant strains grew normally under these conditions [49,51,52]. Accordingly, we checked the ability of the new set of mutants to grow under various experimental conditions. Growth rates under anaerobic or aerobic conditions of the C67S, C70S, C106S and E71K mutants were comparable to that of the wild-type B10 strain (Fig. 2A,B). Under anaerobic conditions, the growth phenotype of these four mutants was clearly distinct from that of the C74S mutant fully defective in Complex I (Fig. 2A).

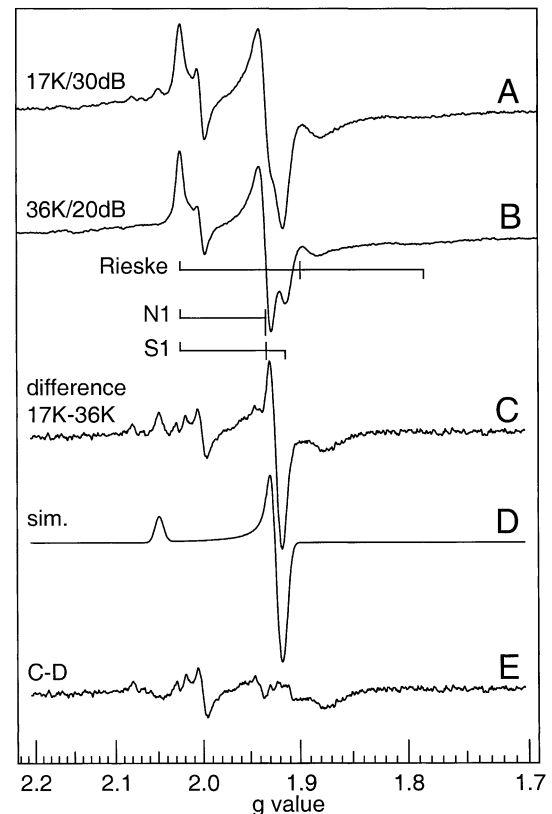


Fig. 3. EPR spectra of fully reduced membranes from B10 cells of *R. capsulatus* at 17 and 36 K, and nonsaturating microwave power. The membranes were reduced with 8 mM succinate for 15 min at 30 °C. Thereafter, 3 mM NADH plus 15 mM dithionite were added, and the sample was frozen in liquid nitrogen after 1 min at 30 °C. (A) Spectrum at 17 K and 30 dB. (B) Spectrum at 36 K and 20 dB. Spectra were normalized with respect to the microwave frequency, microwave power, temperature and gain. (C) Difference A minus B. (D) Simulation of the EPR line shape of the clusters 2 ( $g_{xyz}=1.91586, 1.92491, 2.04795$ ;  $W_{xyz}=1.6, 1.4, 1.55$  mT). (E) Difference C minus D. The traces C to E were two times enlarged relative to the traces A and B. Other EPR conditions: microwave frequency, 9415.6 MHz (normalized value); modulation amplitude, 1.27 mT.

Table 2

NADH- and succinate-oxidase activities of membranes from the mutant and reference strains

Strain	NADH-oxidase activity <sup>a</sup>		Succinate-oxidase activity <sup>a</sup>		Ratio <sup>b</sup>
W1	58	100%	66	100%	0.88
C106S	42	72%	47	71%	0.89
C67S	25	43%	59	89%	0.42
E71K	19	33%	56	85%	0.34
C70S	16	28%	49	74%	0.33
$\Delta nuoI$	8	14%	81	123%	0.10

<sup>a</sup> nmol O<sub>2</sub>/min/mg.

<sup>b</sup> Ratio of the oxidase activities with NADH and succinate. Values are the average from at least three different measurements. W1 is the wild-type reference strain,  $\Delta nuoI$  is a strain deficient in Complex I.

### 3.4. Activities of the respiratory chain

NADH and succinate oxidase activities of membranes of the different mutants are shown in Table 2. In contrast to the C74S mutant, which has no Complex I activity, the C67S, C70S, C106S and E71K mutants showed 28–72% of the wild-type activity. The NADH oxidase activity of the C106S mutant was nearly 30% less than that of the W1 reference strain. For the C67S, C70S and E71K mutants, these activities were still lower, although they remained higher than the activity measured in the membranes of the Complex I depleted  $\Delta nuoI$  mutant. However, in contrast to the basal NADH oxidase activity of the  $\Delta nuoI$  mutant, the NADH oxidase activity supported by the C67S, C70S, E71K and C106S mutant membranes still remained 100% sensitive to piericidin. Succinate oxidase activities were somewhat lower in the mutants, while it was increased in the  $\Delta nuoI$  mutant. Increase in the succinate oxidase activity, while unexplained, has been generally observed in all Complex I deficient *R. capsulatus* mutants [49,51,52].

Taking the ratio between NADH oxidase and succinate oxidase activities as a phenotypic index of the respiratory chain, it is obvious that the C106S mutant behaved like the W1 reference strain, and that the C67S, C70S and E71K

mutants exhibited an intermediate phenotype between wild-type strain and a Complex-I-deficient strain (Table 2). It should be mentioned, however, that the C67S mutant was obtained after complementation of the  $\Delta nuoI$  strain and that  $\Delta nuoI$  complementation with the episomal wild-type *nuoI* gene only concurred to a 70% restoration of the Complex I activity in the B10 strain [49]. Comparison between the  $\Delta nuoI$  strain complemented with the wild-type *nuoI* gene and the C67S mutant would thus allow to assume that the Complex I activity in the C67S mutant was less severely altered than deduced from the values in Table 2. On the other hand, when Complex I activity in the membranes of the different mutants was assayed as the deamino-NADH: ferri-cyanide oxidoreductase activity, the conclusions drawn from the polarographic measurements remained largely valid (not shown). These experiments indicate that four of the mutants (C67S, C70S, E71K and C106S strains) contain partially or nearly fully active Complex I assembled in the membranes.

### 3.5. EPR analysis of membrane preparations

Taking into account the phenotypic features of the different mutants described above, we decided to focus our study on the C67S, C70S, E71K and C106S mutant strains. Iron–

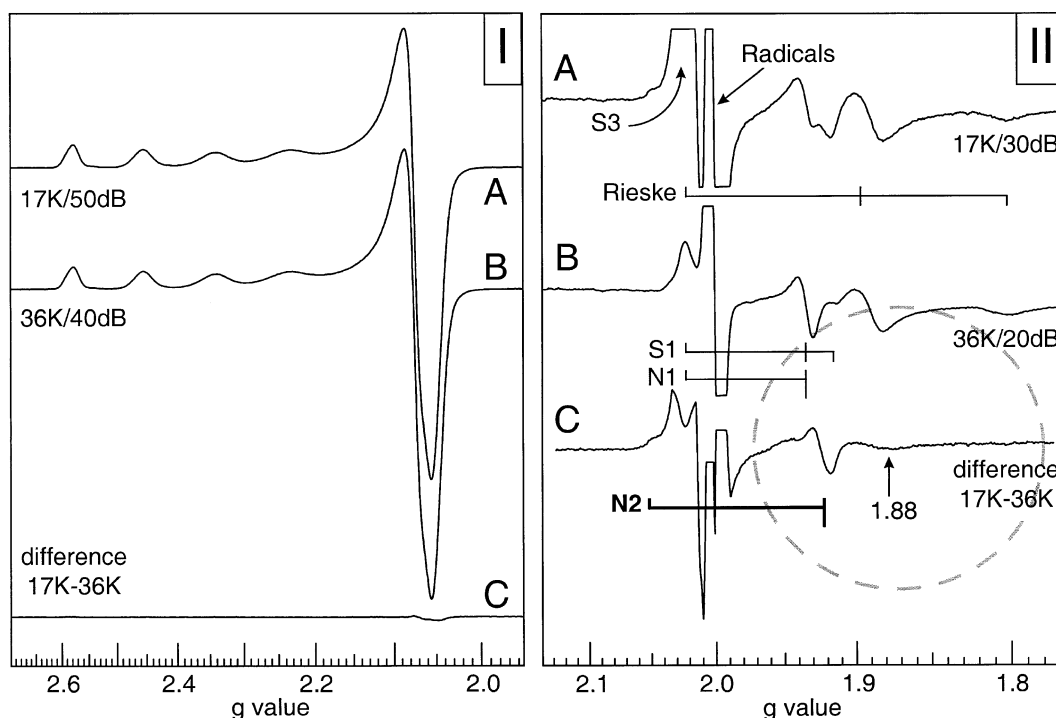


Fig. 4. Panel I: Verification of the spectrometer performance for the comparison of EPR spectra after normalization by using a copper standard (10 mM  $\text{CuSO}_4 \cdot 5\text{H}_2\text{O}$ , 2 M  $\text{NaClO}_4$ , 10 mM HCl). (A) Spectrum of the copper standard at 50 dB and 17 K. (B) Spectrum of the copper standard at 40 dB and 36 K. Spectra were normalized with respect to the microwave frequency, microwave power, temperature and gain. (C) Difference A minus B. Other EPR conditions: microwave frequency, 9424.9 MHz (normalized value); modulation amplitude, 1.27 mT. Panel II: EPR spectra of specifically reduced membranes of W1 cells at 17 and 36 K under nonsaturating conditions. Membrane samples were mixed with 0.2 mM TTFA and 40 mM fumarate. After 30 min on ice, 4 mM NADH was added and the samples were frozen in liquid nitrogen after another 2 min on ice. (A) Spectra recorded at 17 K and 30 dB. (B) Spectra recorded at 36 K and 20 dB. Spectra were normalized with respect to the microwave frequency, microwave power, temperature and gain. (C) Difference A minus B. Other EPR conditions: microwave frequency, 9426.3 MHz; modulation amplitude, 1.27 mT. In the following EPR figures, only the encircled region is shown.

sulfur clusters in Complex I have characteristic features that can be detected by EPR (for an overview, see Ref. [9]). When examining intact membranes of mitochondria or bacteria, a great number of other EPR signals can interfere. As signals from Complex I can be detected only in the reduced complex, membranes have to be reduced by NADH.

In the highly concentrated samples, this will always result in the complete reduction of nearly all components of the respiratory chain.

Some of the initial difficulties encountered in the analysis of the EPR signals of Complex I in *R. capsulatus* membranes are shown in Fig. 3. Trace A is a spectrum, taken at

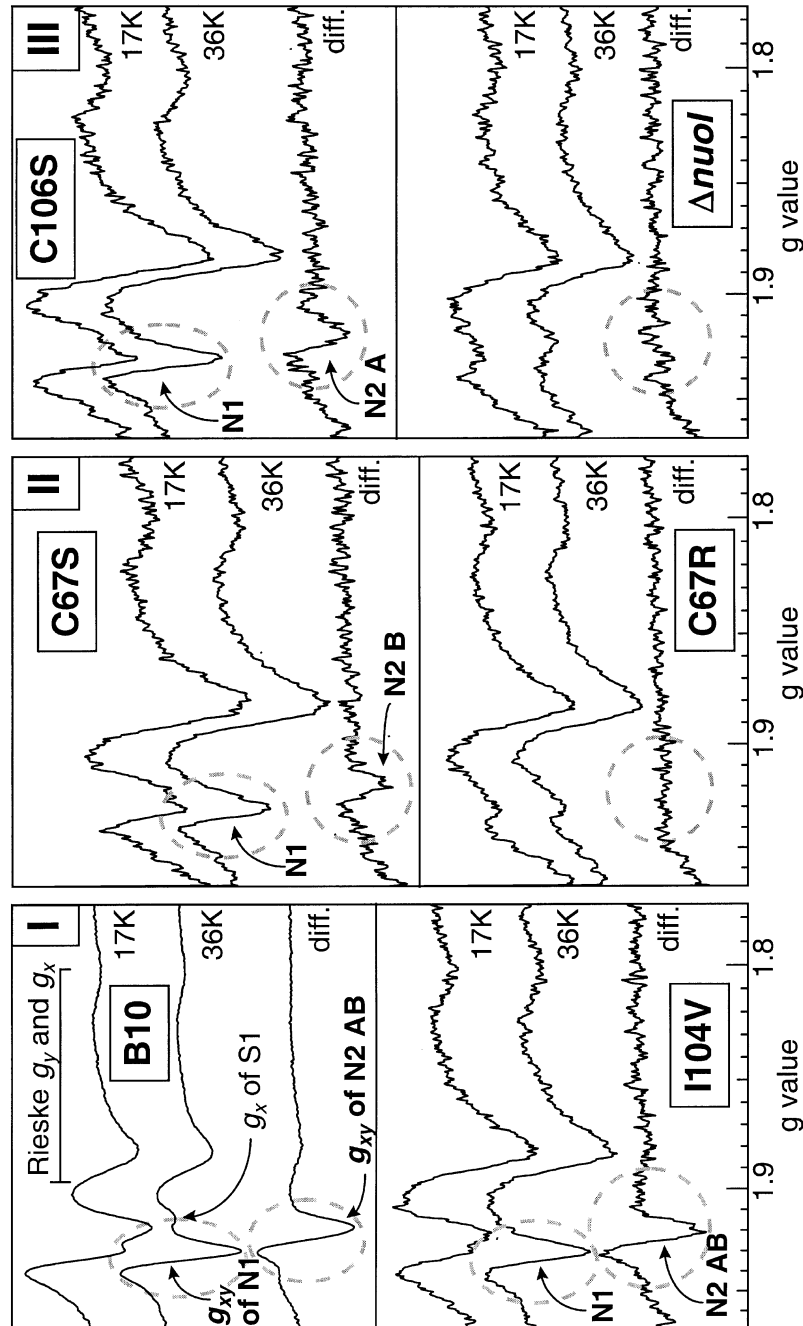


Fig. 5. EPR spectra of specifically reduced membrane samples at 17 and 36 K under nonsaturating conditions. Membrane samples were mixed with 0.2 mM TTFA and 40 mM fumarate. After 30 min on ice, 4 mM NADH was added and the samples were frozen in liquid nitrogen after another 2 min on ice. Only the  $g = 1.97\text{--}1.78$  region of the spectra is shown. Panel I: upper part, B10 membranes; lower part, I104V membranes. Panel II: upper part, C67S membranes; lower part, C67R membranes. Panel III: upper part, C106S membranes; lower part, membranes from cells deficient in Complex I ( $\Delta nuoI$  strain). In each set of three spectra, the upper trace was recorded at 17 K and 30 dB and the middle trace at 36 K and 20 dB. Spectra were normalized for the microwave frequency, microwave power, gain and temperature. The lower traces are the differences A minus B. Other EPR conditions: microwave frequency, 9425.8 MHz; modulation amplitude, 1.27 mT. The presence or absence of EPR signals from Complex I can be seen in the encircled areas.

17 K and nonsaturating microwave power, from membranes of the B10 strain reduced with a mixture of succinate, NADH and dithionite. It shows overlapping signals due to all reduced Fe–S clusters in the sample detectable at 17 K. Trace B is a spectrum at 36 K and nonsaturating power. At this temperature, the EPR signals of the [4Fe–4S] clusters (N2, N3 and N4) are relaxation broadened beyond detection in a first-derivative display, while the signals from the [2Fe–2S] clusters remain still optimally sharpened. The signals of three 2Fe clusters can be recognized: cluster N1 from Complex I, cluster S1 from succinate:ubiquinone oxidoreductase (Complex II) and the Rieske Fe–S cluster from ubiquinol:ferricytochrome *c* oxidoreductase (Complex III). At higher temperatures, the signal from the Rieske Fe–S cluster starts to broaden [53]. At this point, we do not yet know whether the cluster N1a, a [2Fe–2S] cluster, is reducible by NADH or not. In the following, we will refer to the clusters N1a plus N1b as the clusters N1 and to the other clusters as N2, N3 and N4.

As the signals from the 2Fe clusters are also fully present in the 17 K spectra, provided the microwave power is nonsaturating, a difference of the 17 K spectrum minus the 36 K spectrum will produce only the line shapes of the 4Fe clusters detectable at 17 K (trace C). Of course, a normalization for the differences in microwave power, temperature and gain must be performed according to the rules that a signal is proportional to the inverse absolute temperature, the gain and the square-root of the microwave power. This can be written as:

$$I_c = (I_o \cdot T \cdot 10^{(dB/20)})/\text{gain}$$

where  $I_c$  is the corrected intensity,  $I_o$  is the observed (recorded) intensity,  $T$  is the absolute temperature and dB is the relative microwave power read from the spectrometer in dB. In addition, one has to correct for differences in the microwave frequencies [54], as these will shift and shrink or expand experimental spectra on the field scale. One should be aware of the fact that the standard Bruker EPR software for making difference spectra contains an incorrect frequency correction; it only shifts the spectra on a field scale, but does not correct for expansion or shrinkage of the spectra. Because the normalization of the spectra relies on the readings of the spectrometer, the cryostat and microwave frequency counter, one has to ascertain whether these readings are correct. This was verified with spectra of a copper standard (Fig. 4, panel I) likewise recorded at 17 and 36 K. A difference of the normalized spectra is a flat line, showing that the readings of microwave frequency, temperature, gain and relative microwave power are correct.

Returning now to Fig. 3, the main signal in trace C is ascribed to the clusters N2 and can be easily simulated (trace D). At this point, we would like to mention that the Bruker software (WIN-EPR/Win-SimFonia) is unsuited for the simulation of anisotropic  $S=1/2$  EPR spectra because it contains a software error resulting in erroneous line shapes

(S.P.J. Albracht, unpublished observations). The quality of the simulation can be judged by the difference spectrum C minus D in trace E. This trace also shows that the contributions of the clusters N3 and N4 to the spectrum are minimal at this temperature, i.e. they are still quite broad due to their rapid spin-lattice relaxation. We cannot rule out that the residual spectrum also contains contributions from signals of 4Fe clusters in ETF:ubiquinone oxidoreductase (if present in *R. capsulatus* membranes) and Complex II. Such signals are observed in bovine submitochondrial particles [9]. The 4Fe clusters in these enzymes would be reduced by dithionite.

A comparison as shown in Fig. 3 does not yield information on the line shape of the clusters N1. To more directly monitor the signals from Complex I, we have tried to eliminate the signals of the cluster S1 and S2 from Complex II by selective oxidation. The reduced cluster S1 ( $g_{xyz}=1.91, 1.93, 2.02$ ), responsible for the major signal in

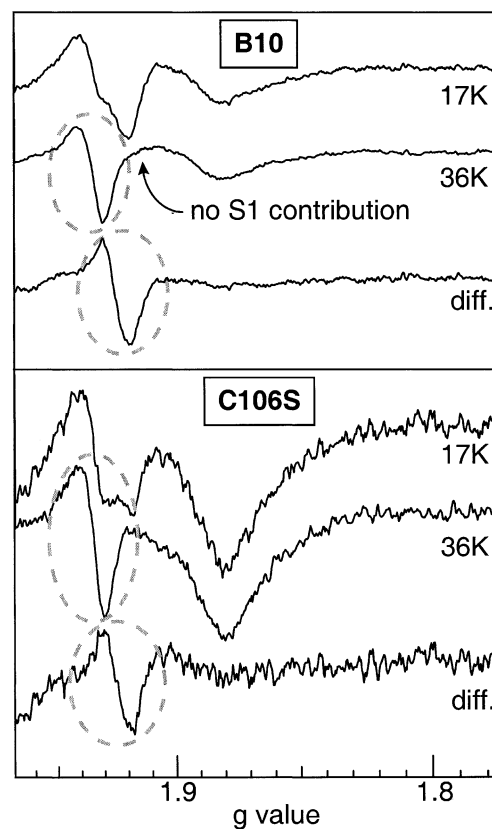


Fig. 6. EPR spectra of specifically reduced membrane samples in the presence of piericidin A at 17 and 36 K under nonsaturating conditions. Membrane samples were mixed with 400 nM piericidin A, 0.2 mM TTFA and 40 mM fumarate. After 30 min on ice, 4 mM NADH was added and the samples were frozen in liquid nitrogen after another 2 min on ice. Only the  $g=1.78$ – $1.97$  region of the spectra is shown. Upper part: B10 membranes. Lower part: C106S membranes. In each part, the upper trace was recorded at 17 K and 30 dB and the middle trace at 36 K and 20 dB. Spectra were normalized for the microwave frequency, microwave power, gain and temperature. The lower traces are the differences 17 K minus 36 K. Other EPR conditions: microwave frequency, 9425.8 MHz; modulation amplitude, 1.27 mT.



trace B of Fig. 3, could be kept oxidized by addition of excess fumarate in the presence of the inhibitor 2-thenoyl-trifluoroacetone (TTFA) and the absence of dithionite (Fig. 4, panel II). Under these conditions, NADH still reduced the Rieske [2Fe–2S] cluster ( $g_{xyz}=2.025$ , 1.89 and 1.8; only the  $g_y$  and  $g_x$  lines are detectable in spectra like these). The 36 K spectrum (trace B) only showed a minimal contribution of the signal from S1 (as observed in the shoulder at  $g_x=1.91$ ), and so the line at  $g=1.94$  was now mainly due to the clusters N1. At 17 K (trace A), the contribution from N2 can clearly be seen. The 17 K minus 36 K difference spectrum (trace C) shows this contribution free of those from reduced 2Fe clusters. The very broad through around  $g=1.88$  is formed by the combined, broadened  $g_x$  lines from the clusters N3 and N4. In the bovine enzyme [9,11], the signals of these cubane clusters need a lower temperature to sharpen up. The spectra in Fig. 4, panel II thus enable a quantitative analysis in terms of reducible 2Fe clusters (N1 in trace B) in Complex I and clusters N2 (in trace C), as elaborated hereafter.

A disadvantage of spectra produced in this way is the presence of very strong, disturbing signals in the  $g=2$  region. They consist of a mixture of sharp radical signals (at  $g=2.003$ ) and, at 17 K, the contribution of the oxidized [3Fe–4S] cluster (cluster S3) from Complex II. In the following figures, we therefore only show the  $g=1.97$ –1.78 region of the spectra (encircled in Fig. 4II, trace C). Fig. 5 shows the 17 K, 36 K and 17 K minus 36 K difference spectra from membranes of the B10, I104V, C67S, C67R, C106S and  $\Delta nuoI$  strains.

The spectra obtained for the B10 and I104V samples (Fig. 5, panel I) show that clear line shapes of the  $g_{xy}$  lines ascribed to clusters N1 and N2 can be obtained. In addition, the  $g_y$  and  $g_x$  lines of the signal from the Rieske Fe–S cluster are present, as well as a very small  $g_x$  line from the S1 of Complex II. When taking the Rieske Fe–S signal as an internal reference, the Complex I content in the I104V membranes was found to be less (44%) than that of wild-type membranes (Fig. 5, panel I). For the B10 and I104V strains, it can be seen (indicated in the encircled areas) that

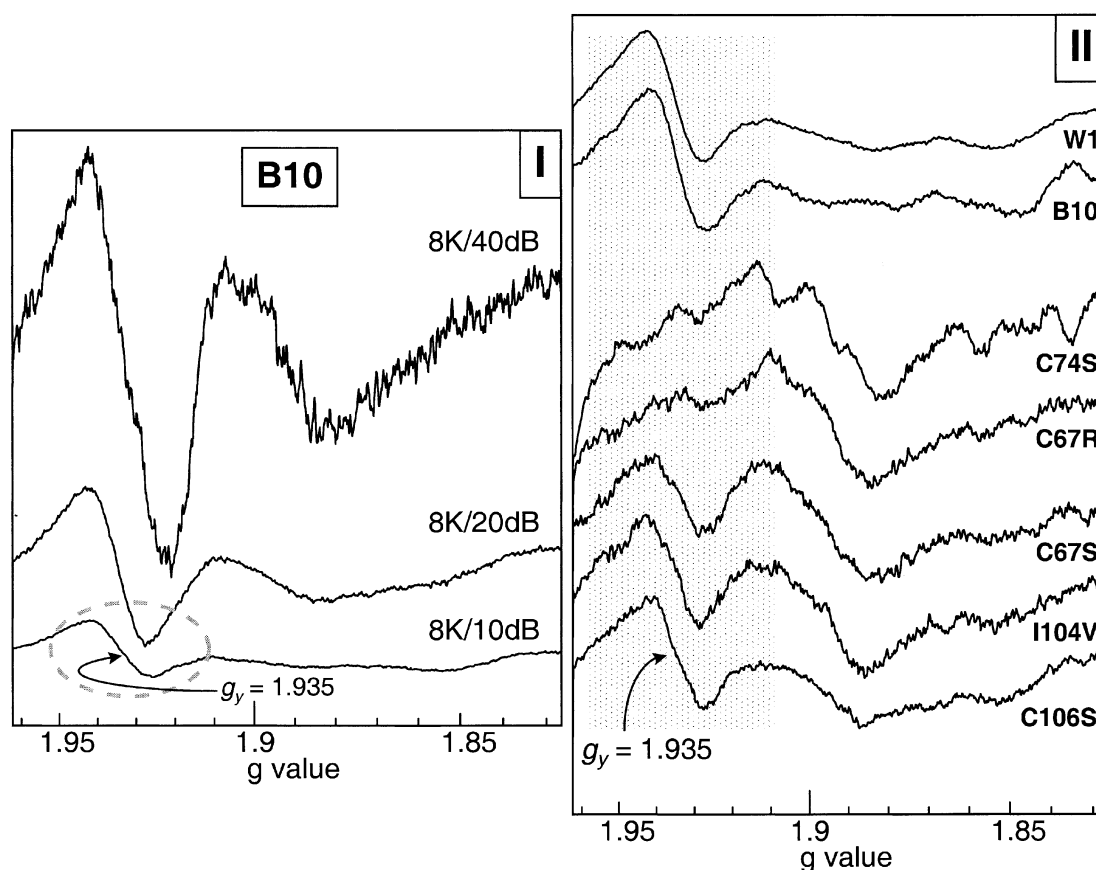


Fig. 7. Detection of the combined  $g_y$  lines of the clusters N3 and N4 by power saturation of the contributions of clusters N1 and N2. Panel I: Membranes of the B10 strain were treated as in Fig. 5. The microwave powers were 40, 20 and 10 dB for the upper, middle and lower traces, respectively. Only the  $g=1.83$ –1.96 region is shown. The traces were normalized for the microwave frequency, microwave power and the gain. Other EPR conditions: microwave frequency, 9421.0 MHz; modulation amplitude, 1.27 mT; temperature, 8 K. Panel II: The combined  $g_y$  lines of the clusters N3 and N4 as detected at 8 K and 10 dB in membranes of *R. capsulatus*. Membranes were treated as in Fig. 5. The figure shows spectra of membranes from (top to bottom) the W1 cells, B10 cells, C74S mutant cells, C67R mutant cells, C67S mutant cells, I104V mutant cells and C106S mutant cells. Only the  $g=1.83$ –1.96 region is shown. All traces were normalized to the same microwave frequency. The  $g_y$  lines of the signals from the clusters N3 plus N4 can be seen in the shaded area. Other EPR conditions: microwave frequency, 9421.0 MHz; modulation amplitude, 1.27 mT.

under the used conditions, the amplitude of the  $g_{xy}$  line from the signal at 36 K due to the clusters N1 (middle traces in each part) is nearly the same as the amplitude of the  $g_{xy}$  line from the signal due to the clusters N2 in the difference spectra (lower traces in each segment). In membranes from the C67S (Fig. 5, panel II) and C106S (Fig. 5, panel III) mutants, however, the relative amplitude of the  $g_{xy}$  line from the signal due to the clusters N2 was about half that of the  $g_{xy}$  line at 36 K from the signals ascribed to the clusters N1. Membranes from the C67R strain and the Complex-I-deficient  $\Delta nuoI$  strain did not show any signal in this region in the 17 K minus 36 K difference spectra. This was also observed with membranes from the C74S strain (not shown). This means that these samples contained no NADH-reducible 4Fe clusters. The samples showed only a minor signal in the  $g=1.94$  region, which was equally intense at 17 and 36 K. This contribution is presumably due to cluster S1 from Complex II, which could not be kept completely oxidized (see also the arrow in trace B in the upper part of Fig. 5, panel I). The fact that the membranes from the C67R, C74S and  $\Delta nuoI$  strains showed a strong Rieske Fe–S signal must mean that these membranes still contained some NADH-dehydrogenase activity. This is in line with residual oxygen-uptake activity (insensitive to piericidin A) with NADH found for these membranes (Table 2). It is less likely that this activity stems from intact Complex I. When membranes of the C67R, C74S and the  $\Delta nuoI$  strains were reduced with succinate, NADH plus dithionite, also no signals due to Complex I were observable (not shown).

When the difference traces (lower traces) of all panel segments were compared, no apparent broadening of the  $g_{xy}$  line from the signal from the clusters N2 could be detected. Fig. 5 thus clearly indicates that the point mutations in the two sets of four conserved Cys residues in the NuoI subunit led either to membranes deficient in Complex I or to a marked decrease (about 50%) in the amplitude of the EPR signal of the clusters N2, relative to that of the clusters N1. Under the used conditions, these ratios were 0.94, 0.48 and 0.46 for the I104V, C67S and C106S mutants, respectively.

### 3.6. Effect of piericidin A on the EPR spectra

In Fig. 5, a very small contribution of the reduced [2Fe–2S] cluster of Complex II (cluster S1) could still be detected at  $g_x=1.91$ . Hence, also the  $g=1.94$  line will receive a contribution from this cluster as its  $g_y$  line is at  $g=1.933$ . Fig. 6 shows that the presence of piericidin A, which blocks electron transfer between Complex I and ubiquinone, in addition to TTFA and fumarate, indeed resulted in the complete disappearance of the signal ascribed to cluster S1.

Hence, the line shape in the  $g=1.92$ – $1.94$  region was now only due to reduced Fe–S clusters of Complex I. The contribution of the Rieske Fe–S cluster was less pronounced than in the absence of piericidin. As before, the ratio of the  $g_{xy}$ -line amplitudes from the signal of the

clusters N2 at 17 K (in the difference spectra) and the signal from the clusters N1 at 36 K was much smaller in the C106S mutant membranes (0.65; lower part of Fig. 6) than in the B10 membranes (1.1; upper part of Fig. 6).

### 3.7. Reduction of the clusters N3 and N4

As remarked above, the contributions of the clusters N3 and N4 to the EPR spectra at 17 K were very weak. We therefore have also recorded spectra at 8 K, where the clusters N3, and one of the clusters N4 [11] in the bovine enzyme, are optimally sharpened. At this temperature, the signals of the 2Fe clusters and the clusters N2 in membranes from B10 cells of *R. capsulatus* were found to saturate very easily. Fig. 7I shows spectra containing the  $g_y$  and  $g_x$  region of the spectra from the Fe–S clusters.

In the upper trace (microwave power 40 dB), all reduced clusters contribute to the spectrum. The middle trace shows the normalized spectrum at 20 dB. If there would be no saturation of any of the signals, the intensity of the spectrum should be identical to the upper trace (compare with the example in Fig. 4, panel I). The fact that this is not so is due to significant saturation of the signals of the cluster N1 and N2 ( $g_{xy}$  lines around  $g=1.935$ ) and the signal of the Rieske Fe–S cluster ( $g_y$  line around  $g=1.89$ ). This effect is even more pronounced in the lower trace recorded at 10 dB (26 mW power incident to the cavity). The remaining line at  $g=1.935$  with a shape, typical for a  $g_y$  line, is nearly solely due to the contributions from the clusters N3 and N4. This line was taken as a (qualitative) measure for the presence of the combined clusters N3 and N4. These clusters have much faster spin-lattice relaxation rates than the other clusters and thus resist microwave-power saturation far better than the clusters N1 and N2.

The relevant part of the spectra from membranes of several strains is shown in Fig. 7II. A  $g_y$  line at  $g=1.935$  can be clearly observed in membranes of the W1, B10,

Table 3

Comparison of the  $g_{xy}$  line amplitudes of signals from the clusters N1 with the  $g_y$  line amplitudes of the combined signals from the clusters N3 plus N4

Sample	Relative amplitudes	
	Clusters N1	Clusters N3 + N4
W1	1	0.93
B10	1	0.99
C74S	absent	absent
C67R	absent	absent
C67S	1	0.92
I104V	1	0.97
C106S	1	0.90

Membrane samples were treated with TTFA, fumarate and NADH as in Fig. 5. The amplitudes of the  $g_{xy}$  lines of the signal from the clusters N1 were measured from spectra recorded at 36 K and 20 dB (nonsaturating). The amplitudes of the  $g_y$  lines of the signals from the clusters N3 plus N4 were measured from spectra recorded at 8 K and 10 dB (Fig. 7II). The amplitudes of the signals due to the combined clusters N3 plus N4 are given relative to those of the  $g_{xy}$  lines of the signal from the clusters N1. For all samples, the same ratio for the gain of the spectra at 36 and 8 K was used.

C67S, I104V and C106S strains (and the E71K strain; not shown), but not in membranes from the strains C74S and C67R (and C64S, C64R, C70S; not shown). To put these results on a more quantitative basis, we have also compared the amplitudes of the  $g_{xy}$  lines of the spectrum of the clusters N1 (at 36 K and 20 dB) with the  $g_y$  lines of the spectra of the combined signals from the clusters N3 plus N4 (at 8 K and 10 dB). The results (Table 3) show that the  $g_y = 1.935$  line as observed at 8 K and high microwave power (10 dB), where the contributions of the signals due to the clusters N1 and N2 are minimized, is equally strong in all samples where Complex I was present. The line was absent in spectra from membranes deficient in Complex I. This means that the cluster N3 and N4 were not affected by the point mutations in the NuoI subunit, unless such a mutation resulted in the lack of Complex I.

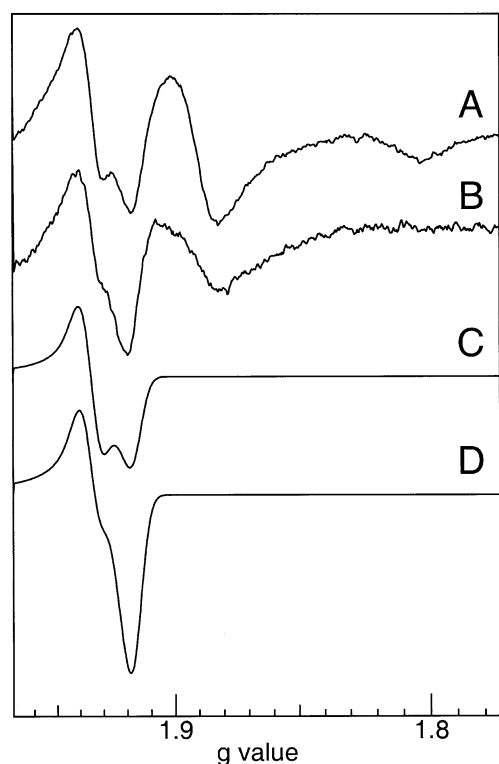


Fig. 8. Estimation of the relative spin concentrations of the NADH-reducible clusters N1 and N2 in membranes from wild-type cells of *R. capsulatus*. (A) The  $g = 1.87$ – $1.97$  region of the spectrum shown in trace A of Fig. 4, panel II. (B) The  $g = 1.87$ – $1.97$  region of the spectrum shown in the upper trace from the upper part of Fig. 6. (C) Summation of the simulated spectra of the clusters N1 and N2 in equal spin concentrations. (D) As C, but now the spin concentration for the clusters N2 was taken twice that of the clusters N1. Simulation parameters, for the clusters N1:  $g_{0z} = 1.92971, 1.93602, 2.01699$  and  $W_{xyz} = 1.43, 1.49, 1.25$  mT (spectrum B in Fig. 4, panel II was taken as the parent spectrum); for the clusters N2:  $g_{0z} = 1.91752, 1.92608, 2.04795$  and  $W_{xyz} = 1.38, 1.45, 1.25$  mT (spectrum C in Fig. 4, panel II was taken as the parent spectrum). The  $g_z$  and  $W_z$  values, which could not be taken from Fig. 4, panel II, were estimated from other (difference) spectra (not shown). Small deviations of these values were of no concern for the line shape in the  $g_{xy}$  region. EPR conditions: microwave frequency, 9426.2 MHz; microwave power, 30 dB; temperature, 17 K; modulation amplitude, 1.27 mT.

### 3.8. NADH can reduce cluster N1a in membrane-bound complex I from *R. capsulatus*

In order to obtain an impression of the relative signal intensities of the signals due to the NADH-reducible 2Fe clusters in Complex I and the signals due to the clusters N2, the simulations shown in Fig. 8 were made.

It can be seen that the simulation in which the relative intensities of both signals were taken equal (trace C) fitted somewhat better to the experimental spectra than the spectrum where the intensity of the signal due to the clusters N2 was twice that of the signal of the 2Fe clusters. This means that, in contrast to the situation in bovine submitochondrial particles [8,43,44], both [2Fe–2S] clusters (N1a and N1b) were nearly completely reduced by NADH in the *R. capsulatus* membranes.

## 4. Discussion

The results of point mutations in subunits from Complex I have been described by a number of groups. When Fe–S clusters were involved, the effects of such mutations on the EPR properties were always studied in the purified complexes, subcomplexes or overexpressed subunits. One of the pitfalls of this approach is that the properties of the purified complex, subcomplex or subunits may considerably deviate from those of the enzyme as present in the membrane. In none of these studies, the EPR spectra of membrane preparations with the modified Complex I have been studied. Likewise, the effects of mutations on the function of Complex I during growth of the parent organism have not been reported. The present study has included both of these important parameters to come to a more reliable assessment of the effects of point mutations in the *nuoI* gene.

### 4.1. Generation of *nuoI* mutants and characterization of their phenotypes

To address the question of the location of the N2 clusters, we have genetically modified the *nuoI* gene, which codes for the NuoI subunit of Complex I in *R. capsulatus* (equivalent to the TYKY subunit in the bovine enzyme). Mutagenesis of the *nuoI* gene involved all the Cys residues (C64, C67, C70 and C74) from the first four-Cys motif, expected to be involved in the coordination of two tetranuclear iron–sulfur clusters (Fig. 1). One Cys residue (C106) of the second four-Cys motif was also included in this study. It must be emphasized that the C64R, C64S, C67R and C67S mutant strains were generated by trans-complementation of a *nuoI* deleted strain. Among these four mutants, only the C67S mutant contained normal amounts of expressed NuoI subunit, which confirms that transcription was efficient in this mutant. However, we cannot rule out the possibility that

expression of the mutated subunit was impaired in the C64R, C64S and C67R mutants because of transcriptional problems. If we assume that mutated *nuoI* genes were correctly transcribed and translated, we can draw a number of interesting conclusions regarding the role of the mutated amino acid residues of NuoI from the immunoassays and enzymatic analysis of the membranes from the mutants reported above.

Cys-64 appears as a very important amino acid that cannot be changed either in Ser or Arg. Similarly, replacement of Cys-67 by an Arg also led to a lack of assembly of Complex I. The C64R, C64S and C67R mutants contained even lower amounts of NuoI than the previously reported C74S mutant [49]. As the two sets of CxxCxxCxxxCP motifs in the NuoI subunit are highly conserved among 2[4Fe–4S] proteins, it is reasonable to assume that C64, C67 and C70 are coordinating one cubane cluster, whereas C74 is coordinating the second cubane (Fig. 1). Hence, the results with the C64S and C74S mutants already point to the presence of two [4Fe–4S] clusters. We conclude that the assembly of both these clusters is a prerequisite for an intact NuoI subunit and apparently also for a correct assembly of Complex I.

Cys-70 also seems to play an important role because its substitution by a Ser was associated with a decreased amount of expressed protein and a poor enzymatic activity (and a lack of EPR signals from Complex I in membrane preparations). The Glu-71 residue is conserved in all NADH:ubiquinone oxidoreductases known [29]. Membranes of the E71K mutant contained quite normal amounts of the NuoI subunit, but they exhibited only a low Complex I activity. Finally, in the case of the C67 and C106 Cys residues, their substitution by Ser residues also caused a decrease of the Complex I activity in the resulting mutants. The decreased content of Complex I in the membranes is considered to be the main factor for the lower activities in the mutants. We note that the growth of *R. capsulatus* strains under anaerobic, photosynthetic conditions can be sustained by a Complex I with the C67S, E71K and C106S mutations in the TYKY subunit. This demonstrates that the energy-dependent reduction of  $\text{NAD}^+$  is still carried out by the enzyme in these mutants.

## 4.2. EPR spectra

### 4.2.1. NADH reduces both [2Fe–2S] clusters in the membrane-bound enzyme

EPR analysis of the membranes from B10 and W1 cells, combined with computer simulations (Fig. 8), indicate that the signals from Complex I at 17 K consist of a nearly equal contributions (double-integrated intensity) of signals from [2Fe–2S] clusters (N1) and from [4Fe–4S] clusters (N2). In the bovine enzyme, the signal of the NADH-reducible 2Fe clusters (N1b) has an intensity half that of the signal of the clusters N2 [43,44]. Complex I subunits containing a binding motif for a 2Fe cluster are

the 75 kDa (NuoG) and the 24 kDa (NuoE) subunits [16,22]. As demonstrated in this study, the NuoI subunit contains two cubane clusters. This means that if the subunits NuoE, NuoG and NuoI are present in equal amounts, then both the NuoE and NuoG subunits contain a [2Fe–2S] cluster in the membrane-bound *R. capsulatus* Complex I and both are reduced by NADH under the present conditions.

### 4.2.2. Effect of nondestructive mutations on the EPR signal ascribed to the clusters N2

Membranes of the I104V mutant cells, as well as from the C67S and C106S mutant cells, showed an EPR signal from the N1 clusters that was about 44% of the intensity of that of B10 or W1 cells. While the N2/N1 ratio in the I104V mutant was the same as in the B10 and W1 cells, this ratio was about 50% lower in the membranes from the C67S and C106S mutant cells. As the latter mutant cells still showed a normal photosynthetic growth behaviour (Fig. 2) and NADH-oxidase activities (Table 2), it is concluded that Complex I is still intact and that it possesses a NuoI subunit with one normal ( $S=1/2$ ), EPR-detectable [4Fe–4S] cluster, giving rise to half the normal signal intensity (labelled as N2 A or N2 B in Figs. 1 and 5), and one Fe–S cluster that was not detectable in the  $g=2$  region. Replacement of the Cys-67 residue by an Arg resulted in membranes lacking Complex I. Therefore, we conclude that in the C67S and C106S mutants, the introduced Ser residue is a direct ligand to one (termed N2 A in Figs. 1 and 5) or the other (termed N2 B in Figs. 1 and 5) [4Fe–4S] cluster, respectively, and that these modified clusters are still functional. When reduced, their EPR signals must have considerably changed because they do not contribute to the signal of the other, normal cluster N2 (Fig. 5). As described below, we tentatively assume that the modified clusters are  $S=3/2$  systems. We note that both Cys residues, C67 and C106, are centred between two other Cys residues in the CxxCxxC parts of the two four-Cys motifs in the amino acid sequence of the NuoI subunit. As this CxxCxxC structure forms a sort of ‘clamp’ around the clusters (Figs. 1 and 9), a weakened ligand at either end may explain the instability of the C64S and C70S mutants and the relative stability of the C67S and C106S mutant enzymes.

Membranes of the E71K mutant cells gave EPR spectra where the amplitude of the  $g=1.94$  signal from the clusters N1 was about 40% of the amplitudes found in the I104V and C106S mutant membranes (and thus less than 20% of  $g=1.94$  amplitude in the B10 membranes); the signal of the Rieske Fe–S cluster was taken as an internal standard. The weak EPR signals made a precise spectroscopic analysis rather difficult. Yet, from the EPR line shape in the  $g=1.92$ – $1.94$  region, it could be seen that the relative ratio of the signals from the clusters N2 and N1 resembled that in the B10 cells and was certainly higher than the ratio found in the C106S mutant membranes. This indicates that both clusters N2 were present in an apparently unperturbed state.



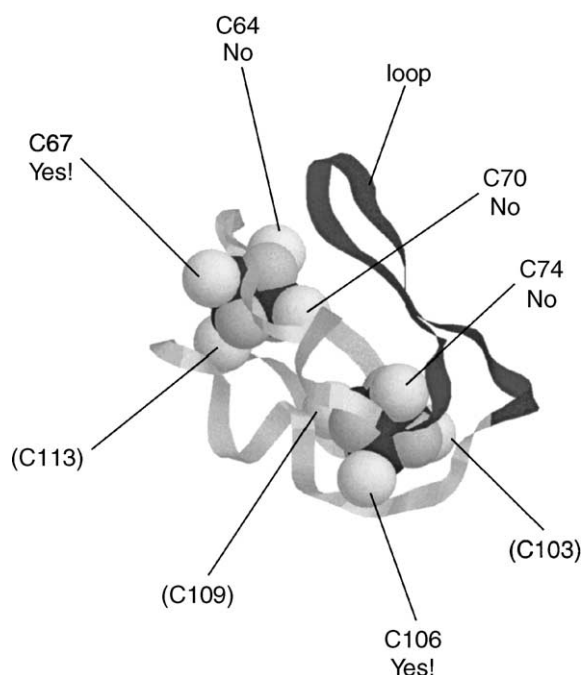


Fig. 9. Summarizing picture visualizing the Cys to Ser point mutations in the NuoI subunit studied in this paper. The structure of ferredoxin from *P. asaccharolyticus* (formerly *Peptococcus aerogenes*) was used as a template (1dur; replacement for 1fdx [72]). The loop between the two four-Cys motifs in the amino acid sequence is shown in dark grey; this loop involves 17 amino acids in the *P. asaccharolyticus* Fd, but 27 residues in the NuoI subunit. The mutations C64S, C70S and C74S did not result in an EPR-detectable Complex I in membrane preparations and are marked as 'No'. The mutations C67S and C106S resulted in a functional Complex I and are marked as 'Yes!'. Mutation of the other three Cys residues has not been tried.

The mutation of the E71 residue may influence the properties of (one of) the Fe–S clusters. Replacement of the negative charge of the Glu residue by the positive charge of the Lys residue could affect the electronic environment of (one of) the iron–sulfur cluster.

Kowal et al. [55] have performed Cys to Ser point mutations for the ligands of the 4Fe cluster in fumarate reductase from *E. coli*. The structure of this enzyme is probably very similar to the crystal structure of the enzyme from *Wolinella succinogenes* [56]. A Cys to Ser mutation of the central Cys residue in the CxxCxxC motif resulted in a cluster with a  $S = 3/2$  ground state (and a decrease of 72 mV of its redox potential). The EPR signature of this state, with broad lines at  $g = 5$  and 5.7, was only very weak. A Cys to Ser mutation of the first Cys residue produced a cluster with a  $S = 1/2$  ground state (and a 60 mV lower redox potential). Mutation of the third and fourth Cys residues in the CxxCxxC- $x_n$ -C motif did not lead to an assembled Fe–S cluster. If a  $S = 3/2$  EPR signal, with the main lines around  $g = 5$ , would be present in Complex I in the membrane preparations of *R. capsulatus*, it would go unnoticed due to the low concentrations of Complex I attainable in EPR samples of such membranes.

Studies with the two [4Fe–4S] clusters in the Psac subunit of the Photosystem I of *Synechococcus* sp. strain

PCC 7002 showed that substitutions of the second Cys of the first or second CxxCxxCxxxCP motif by Ser, Ala or Asp residues allowed the protein to refold with two iron–sulfur clusters: one [4Fe–4S] cluster ( $S = 1/2$ ) and one [3Fe–4S] cluster. The C  $\rightarrow$  S and C  $\rightarrow$  A mutant proteins could still bind to a PSI complex [57]. Mutation of the fourth Cys residue into Asp likewise changed one of the clusters into a 3Fe cluster. Mutagenesis studies with ferredoxin I from *Azotobacter vinelandii* showed that the [4Fe–4S] cluster in this protein prefers a coordination with four Cys ligands [58,59]. When the first Cys residue in the CxxxC- $x_n$ -CxxCxxC motif, which together with the last three Cys residues coordinates the cluster in the wild-type protein, was changed to either Ala or Ser, an intact cluster was formed using the second Cys residue in the motif. In general, the structural and functional impacts of Cys substitutions in iron–sulfur proteins are difficult to predict (for review, see Ref. [60]).

#### 4.2.3. The C67S and C106S mutations did not effect the clusters N1, N3 and N4

The relative EPR intensities of the 2Fe clusters and the clusters N3 plus N4 in membranes from the C67S and C106S cells were the same as found in membranes of the B10, W1 and I104V cells (Fig. 7II and Table 3). This means that these point mutations did not affect these clusters.

#### 4.2.4. Effect of the other mutations

No EPR signals from Complex I could be detected in the membrane preparations from the C64R, C64S, C67R and C74S mutant cells. We conclude that in each mutant, one of the Fe–S clusters in the NuoI subunit could not be stabilized. The resulting NuoI subunit could not be used by the mutant cells for the assembly of an intact, membrane-bound Complex I. The C70S mutants cells showed quite a normal growth (Fig. 2), but their membranes had only a low NADH-oxidase activity and lacked detectable EPR signals from Complex I. Apparently, the C70S mutation considerably weakens the structural stability of Complex I.

#### 4.2.5. Earlier evidence pointing to two clusters N2 (N2a and N2b)

The first indications for the existence of two clusters N2 came from studies on the bovine enzyme published more than two decades ago [43]. This was later reinforced by detailed analyses of EPR spectra [44] where it was shown that quantitative interpretations by other workers were in error. The first indication for two kinetically distinguishable clusters N2 was already described in 1982 [61]. Abundant evidence reinforcing this behaviour was subsequently published [42,62,63]. Also, inhibitor studies with piericidin [64] clearly showed that full inhibition of Complex I can, under certain conditions, be accomplished by one molecule of piericidin per two clusters N2. Energy-induced exchange coupling between the two clusters has been discovered in tightly coupled submitochondrial particles [38,65]. This

phenomenon was uncoupler sensitive. This all has led to a model of a Complex I molecule with two clusters N2 (N2a and N2b) [11], in which these Fe–S clusters were proposed to play a vital role in the electrons-transfer driven proton translocation [29].

The presence of two tetranuclear iron–sulfur clusters in the TYKY subunit was anticipated as soon as the discovery of this subunit in the bovine Complex I because of similarities of the primary sequence with 2[4Fe–4S] bacterial ferredoxins [39]. The data presented here provide the first experimental evidence for this hypothesis. A picture summarizing the present results is shown in Fig. 9.

The structure also highlights the stretch of amino acids between the third and the fourth Cys residue coordinating one of the [4Fe–4S] clusters. This stretch is 17 residues long in the *Peptostreptococcus asaccharolyticus* ferredoxin (taken as example in Fig. 9), but involves 27 residues in all NADH:ubiquinone oxidoreductases and 28 residues in the NADH:plastoquinone oxidoreductases [29].

#### 4.2.6. Comparison of our results with effects of point mutations on the EPR signal of N2 reported by other groups

Based on the growing awareness of analogies in the amino acid sequences of subunits from Complex I and [NiFe]-hydrogenases [11,25,26,66,67], it was proposed that the 49 kDa subunit, the PSST subunit and the TYKY subunit have an intimate and essential contact [29]. Especially, the highly conserved stretch of amino acids between the two four-Cys motifs in the sequence of the NuoI (TYKY) subunits in all Complexes I, which in normal 2[4Fe–4S] ferredoxins forms a loop (17 residues in the example in Fig. 9) on the outside of the protein, suggests that this part of the TYKY subunit may be very important for the binding to the 49-kDa PSST couple. We therefore expect that the properties of the clusters N2a and N2b are critically dependent on a correct structure of each of the three subunits in the 49-kDa PSST-TYKY functional unit. Indeed, the 4Fe clusters in an overexpressed, truncated form of the Nqo9 (TYKY) subunit of *P. denitrificans* reconstituted with iron and sulfide have a midpoint potential ( $< -600$  mV) very much lower than that of the N2 cluster(s) in the membrane-bound complex [40]. Incidentally, the  $g$  values of one of the two EPR signals in the spectrum of this overexpressed protein ( $g_{xyz} = 1.92, 1.92, 2.05$ ) were similar to those of the N2 signal found in the membrane-bound complex [68,69].

Certain point mutations in the 49-kDa subunit of Complex I from *Y. lipolytica* [20], a subunit without any conserved Cys residues, resulted in the decrease or the complete loss of the EPR signal ascribed to cluster N2 in the purified enzyme reduced with NADH. EPR signals of the other clusters were apparently unperturbed, so the assembly of the Complex was not affected in these mutants. The authors assumed that the PSST subunit hosted ‘cluster N2’ and provided three Cys residues as

ligands. They speculated that the fourth ligand for this cluster may be provided by a residue from the 49-kDa subunit, although they could not tell which one. An earlier proposal that a specific Glu residue in the 49-kDa subunit might function as the fourth ligand for an Fe–S cluster in the PSST subunit [41] was excluded by point-mutation studies [18].

We note that the results from experiments in the present paper and the accompanying paper [30] clearly demonstrate that there are two  $S = 1/2$  systems with a very similar line shape contributing to the EPR signal ascribed to cluster N2 in the bovine and *R. capsulatus* enzymes. Hence, in these enzymes, the PSST subunit cannot be the site of binding, as this subunit contains Cys residues for the binding of at most one cluster. The present paper shows that both clusters N2 are located in the NuoI (TYKY) subunit. We explain the results obtained with mutations in the 49-kDa subunit of Complex I from *Y. lipolytica* [20] by a disturbance of the delicate interactions within the 49-kDa PSST-TYKY subunits, resulting in an altered level of reduction of the N2 clusters in the TYKY subunit. This may be a change in the redox potential, a disturbance of electron transfer or a combination of the two. We note that it is very likely that the two [4Fe–4S] clusters are still present in TYKY subunit of the mutated, purified Complex I preparations from *Y. lipolytica* [20], as our study demonstrates that assembly of *R. capsulatus* Complex I is not possible when one of the clusters is missing.

Mutations of an E or D residue (D136N and E140Q) in the PSST homologue in *Y. lipolytica* resulted in an altered line shape of the EPR signal of cluster N2 (broadening of the  $g_z$  line) [18]. Also, point mutations in the PSST subunit of the *N. crassa* enzyme [17] dramatically affected the EPR signal ascribed to cluster N2. From two strains in which two different point mutations in the PSST subunit were induced, a Complex I was purified, which did not show the EPR signal of N2 in enzyme reduced with excess NADH in the presence of redox mediators. The two *N. crassa* enzymes, one with a C101S mutation and the other with a C102A mutation in the PSST subunit, showed small but distinct differences in their EPR signals from the remaining clusters at  $g$  values, around 2.04 and 1.92, where contributions of the clusters N3 are expected. Regrettably, the authors did not comment on these differences. Also in this case, we explain the data as a disturbance of the fragile structure of the 49-kDa PSST-TYKY subunits resulting in altered properties of the clusters N2 in the TYKY subunit. The differences in the EPR spectra of the two mutant enzymes may well be the first indication that the PSST subunit harbours a [4Fe–4S] cluster with  $g$  values similar to one of the two clusters N3. The line shapes of the clusters N3a and N3b in Complex I have not yet been established in detail.

The data here and in the accompanying paper [30] likewise show that the proposal [70] that the TYKY subunit

would contain two reducible, thus far EPR-undetected [4Fe–4S] clusters (N6a and N6b) does not hold for the bovine and *R. capsulatus* enzymes.

## Acknowledgements

This study was supported by the Région Rhône-Alpes Vieillessement and by EU Grant BIO2-CT93-0364. Drs. J. Meyer and J. Gaillard are acknowledged for helpful discussions.

## References

- [1] J.E. Walker, Q. Rev. Biophys. 25 (1992) 253–324.
- [2] I.M. Fearnley, J. Carroll, R.J. Shannon, M.J. Runswick, J.E. Walker, J. Hirst, J. Biol. Chem. 276 (2001) 38345–38348.
- [3] T. Friedrich, Biochim. Biophys. Acta 1364 (1998) 134–146.
- [4] K. Leonard, H. Haiker, H. Weiss, J. Mol. Biol. 194 (1987) 277–286.
- [5] V. Guénebaud, A. Schlitt, H. Weiss, K. Leonard, T. Friedrich, J. Mol. Biol. 276 (1998) 105–112.
- [6] N. Grigorieff, J. Mol. Biol. 277 (1998) 1033–1046.
- [7] B. Bottcher, D. Scheide, M. Hesterberg, L. Nagel-Steger, T. Friedrich, J. Biol. Chem. 277 (2002) 17970–17977.
- [8] T. Ohnishi, H. Blum, Y.M. Galante, Y. Hatefi, J. Biol. Chem. 256 (1981) 9216–9220.
- [9] H. Beinert, S.P.J. Albracht, Biochim. Biophys. Acta 683 (1982) 245–277.
- [10] H. Leif, V.D. Sled, T. Ohnishi, H. Weiss, T. Friedrich, Eur. J. Biochem. 230 (1995) 538–548.
- [11] S.P.J. Albracht, A.M.P. De Jong, Biochim. Biophys. Acta 1318 (1997) 92–106.
- [12] A.B. Kotlyar, S.P.J. Albracht, R.J.M. Van Spanning, Biochim. Biophys. Acta 1365 (1998) 53–59.
- [13] T. Ohnishi, V.D. Sled, T. Yano, T. Yagi, D.S. Burbaev, A.D. Vinogradov, Biochim. Biophys. Acta 1365 (1998) 301–308.
- [14] C.I. Ragan, Y.M. Galante, Y. Hatefi, T. Ohnishi, Biochemistry 21 (1982) 590–594.
- [15] T. Yagi, T. Yano, S. Di Bernardo, A. Matsuno-Yagi, Biochim. Biophys. Acta 1364 (1998) 125–133.
- [16] A. Dupuis, M. Chevallet, E. Darrouzet, H. Duborjal, J. Lunardi, J.P. Issartel, Biochim. Biophys. Acta 1364 (1998) 147–165.
- [17] M. Duarte, H. Populo, A. Videira, T. Friedrich, U. Schulte, Biochem. J. 364 (2002) 833–839.
- [18] P.M. Ahlers, K. Zwicker, S. Kerscher, U. Brandt, J. Biol. Chem. 275 (2000) 23577–23582.
- [19] N. Kashani-Poor, S. Kerscher, V. Zickermann, U. Brandt, Biochim. Biophys. Acta 1504 (2001) 363–370.
- [20] N. Kashani-Poor, K. Zwicker, S. Kerscher, U. Brandt, J. Biol. Chem. 276 (2001) 24082–24087.
- [21] S. Kerscher, S. Drose, K. Zwicker, V. Zickermann, U. Brandt, Biochim. Biophys. Acta 1555 (2002) 83–91.
- [22] I.M. Fearnley, J.E. Walker, Biochim. Biophys. Acta 1140 (1992) 105–134.
- [23] J.E. Walker, J.M. Skehel, S.K. Buchanan, Methods Enzymol. 260 (1995) 14–34.
- [24] T. Yagi, T. Yano, A. Matsuno-Yagi, J. Bioenerg. Bioembranes 25 (1993) 339–345.
- [25] S.P.J. Albracht, Biochim. Biophys. Acta 1144 (1993) 221–224.
- [26] S.P.J. Albracht, Biochim. Biophys. Acta 1188 (1994) 167–204.
- [27] A. Volbeda, M.H. Charon, C. Piras, E.C. Hatchikian, M. Frey, J.C. Fontecilla-Camps, Nature 373 (1995) 580–587.
- [28] A. Volbeda, E. Garcia, C. Piras, A.L. deLacey, V.M. Fernandez, E.C. Hatchikian, M. Frey, J.C. Fontecilla-Camps, J. Am. Chem. Soc. 118 (1996) 12989–12996.
- [29] S.P.J. Albracht, R. Hedderich, FEBS Lett. 485 (2000) 1–6.
- [30] S.P.J. Albracht, E. Van der Linden, B. Faber, Biochim. Biophys. Acta 1557 (2002) [this issue](#).
- [31] J.W. Peters, W.N. Lanzilotta, B.J. Lemon, L.C. Seefeldt, Science 282 (1998) 1853–1858.
- [32] T. Yano, T. Yagi, V.D. Sled, T. Ohnishi, J. Biol. Chem. 270 (1995) 18264–18270.
- [33] T. Yano, V.D. Sled, T. Ohnishi, T. Yagi, Biochemistry 33 (1994) 494–499.
- [34] T. Yano, V.D. Sled, T. Ohnishi, T. Yagi, J. Biol. Chem. 271 (1996) 5907–5913.
- [35] P. Wilks, J.E. Walker, S.P.J. Albracht, R. Van Belzen, Protein Sci. 4 (Suppl. 1) (1995) 61.
- [36] W. Fecke, V.D. Sled, T. Ohnishi, H. Weiss, Eur. J. Biochem. 220 (1994) 551–558.
- [37] U. Brandt, Biochim. Biophys. Acta 1318 (1997) 79–91.
- [38] R. Van Belzen, A.B. Kotlyar, N. Moon, W.R. Dunham, S.P.J. Albracht, Biochemistry 36 (1997) 886–893.
- [39] A. Dupuis, J.M. Skehel, J.E. Walker, Biochemistry 30 (1991) 2954–2960.
- [40] T. Yano, S. Magnitsky, V.D. Sled, T. Ohnishi, T. Yagi, J. Biol. Chem. 274 (1999) 28598–28605.
- [41] T. Ohnishi, J. Bioenerg. Bioembranes 25 (1993) 325–329.
- [42] R. Van Belzen, S.P.J. Albracht, Biochim. Biophys. Acta 974 (1989) 311–320.
- [43] S.P.J. Albracht, F.J. Leeuwerik, B. Van Swol, FEBS Lett. 104 (1979) 197–200.
- [44] R. Van Belzen, A.M.P. De Jong, S.P.J. Albracht, Eur. J. Biochem. 209 (1992) 1019–1022.
- [45] Y. Hatefi, A.G. Haavik, D.E. Griffiths, J. Biol. Chem. 237 (1962) 1667–1680.
- [46] T. Cremona, E.B. Kearney, J. Biol. Chem. 239 (1964) 2328–2334.
- [47] C.J. Lusty, J.M. Machinist, T.P. Singer, J. Biol. Chem. 240 (1965) 1804–1810.
- [48] C. Paech, J.R. Reynolds, T.P. Singer, R.H. Holm, J. Biol. Chem. 256 (1981) 3167–3170.
- [49] M. Chevallet, A. Dupuis, J. Lunardi, R. Van Belzen, S.P.J. Albracht, J.P. Issartel, Eur. J. Biochem. 250 (1997) 451–458.
- [50] P.F. Weaver, J.D. Wall, H. Gest, Arch. Microbiol. 105 (1975) 207–216.
- [51] A. Dupuis, A. Peinnequin, E. Darrouzet, J. Lunardi, FEMS Microbiol. Lett. 148 (1997) 107–114.
- [52] J. Lunardi, E. Darrouzet, A. Dupuis, J.P. Issartel, Biochim. Biophys. Acta 1407 (1998) 114–124.
- [53] S. De Vries, S.P.J. Albracht, F.J. Leeuwerik, Biochim. Biophys. Acta 546 (1979) 316–333.
- [54] S.P.J. Albracht, in: C.P. Lee (Ed.), Current Topics in Bioenergetics, vol. 13, Academic Press, New York, 1984, pp. 79–106.
- [55] A.T. Kowal, M.T. Werth, A. Manodori, G. Cecchini, I. Schröder, R.P. Gunsalus, M.K. Johnson, Biochemistry 34 (1995) 12284–12293.
- [56] C.R.D. Lancaster, A. Kröger, M. Auer, H. Michel, Nature 402 (1999) 377–385.
- [57] T. Mehari, F. Qiao, M.P. Scott, D.F. Nellis, J. Zhao, D.A. Bryant, J.H. Golbeck, J. Biol. Chem. 270 (1995) 28108–28117.
- [58] S.E. Iismaa, A.E. Vazquez, G.M. Jensen, P.J. Stephens, J.N. Butt, F.A. Armstrong, B.K. Burgess, J. Biol. Chem. 266 (1991) 21563–21571.
- [59] B. Shen, D.R. Jollie, T.C. Diller, C.D. Stout, P.J. Stephens, B.K. Burgess, Proc. Natl. Acad. Sci. U. S. A. 92 (1995) 10064–10068.
- [60] J.M. Moulis, V. Davaise, M.P. Golinelli, J. Meyer, I. Quinkal, J. Biol. Inorg. Chem. 1 (1996) 2–14.
- [61] S.P.J. Albracht, in: V. Massey, C.H. Williams (eds.), Flavins and Flavoproteins, Elsevier/North-Holland, New York, 1982, pp. 759–762.
- [62] P.T. Bakker, S.P.J. Albracht, Biochim. Biophys. Acta 850 (1986) 413–422.

- [63] S.P.J. Albracht, P.T. Bakker, *Biochim. Biophys. Acta* 850 (1986) 423–428.
- [64] R. Van Belzen, M.C. Van Gaalen, P.A. Cuypers, S.P.J. Albracht, *Biochim. Biophys. Acta* 1017 (1990) 152–159.
- [65] A.M.P. De Jong, A.B. Kotlyar, S.P.J. Albracht, *Biochim. Biophys. Acta* 1186 (1994) 163–171.
- [66] S.J. Pilkington, J.M. Skehel, R.B. Gennis, J.E. Walker, *Biochemistry* 30 (1991) 2166–2175.
- [67] R. Böhm, M. Sauter, A. Böck, *Mol. Microbiol.* 4 (1990) 231–243.
- [68] S.P.J. Albracht, H.W. Van Verseveld, W.R. Hagen, M.L. Kalkman, *Biochim. Biophys. Acta* 593 (1980) 173–186.
- [69] S.W. Meinhardt, T. Kula, T. Yagi, T. Lillich, T. Ohnishi, *J. Biol. Chem.* 262 (1987) 9147–9153.
- [70] T. Rasmussen, D. Scheide, B. Brors, L. Kintscher, H. Weiss, T. Friedrich, *Biochemistry* 40 (2001) 6124–6131.
- [71] B. Marrs, *Proc. Natl. Acad. Sci. U. S. A.* 71 (1974) 971–973.
- [72] E.T. Adman, L.C. Sieker, L.H. Jensen, *J. Biol. Chem.* 248 (1973) 3987–3996.